2018 IEEE International Conference on Robotics and Automation (ICRA)
May 21-25, 2018, Brisbane, Australia

High Speed Whole Body Dynamic Motion Experiment with Real Time Master-Slave Humanoid Robot System

Yasuhiro Ishiguro and Kunio Kojima and Fumihito Sugai and Shunichi Nozawa
and Yohei Kakiuchi and Kei Okada and Masayuki Inaba

Abstract— **In this paper, we propose novel methods suitable for online real time whole body master-slave control with real life-sized humanoid robot. We conducted some dynamic whole body master-slave experiment with life-sized humanoid robot, and we achieved speedier and flexible master-slave operation compared to conventional study. Conventionally, master-slave operations with humanoid robots were available with only the upper body of the humanoid robot , and the COM movement was limited to be static. In our previous study, we introduced LIP model based restrictions to ensure the balance stability. In this study, we extend the safety restrictions by introducing foot landing delay prediction and trajectory smoothing method suitable for real robot. We conducted master-slave tennis swing experiment and high kick motion experiment with life-sized humanoid robot "JAXON", and we evaluated the effectiveness of our proposed methods and system.**

I. Introduction

One of the most remarkable use of a humanoid robot is utilizing its machine body as a substitute of our own body. Conventionally, in the case of object manipulation or picking tasks, arm type robots or cart type robots are suitable rather than humanoid robots. However, in case of playing speedy or dexterous whole body motions e.g. emergency tasks or sports motions, only humanoid robot can play such motions. If we complete the real-time whole body master-slave tele-operation system for humanoid robot, such a system will be the most maneuverable tele-operation system for human being.

Conventional researches about humanoid tele-operation use joysticks or GUIs to control the positions of the end effectors or walking direction [1], [2], [3], [4]. For more intuitive and dexterous maneuver, resent researchers use motion capture system or wearable devices to get operator's posture, and first, they apply the posture to the humanoid upper body [5], [6], [7]. Even in the whole body cases, they only allows the static movement of Center Of Mass (COM) [8], [9], [10], [11]. These study cases were not able to execute dynamic whole body motions using all Degree Of Freedom (DOF) in the life-sized bipedal humanoid robot in real time.

The most difficult point of real time master-slave humanoid control is treating the risk of falling down due to its two legs. Previous conventional studies restrained the risk by applying conservative restrictions to the relation between COM and foot support region. In our previous works [12], [13], we achieved non-static bipedal humanoid locomotion with master-slave approach with Liner Inverted Pendulum dynamics model [14], [15] based restrictions.

Fig. 1. An extreme example of a real time, whole body, dynamic, master-slave operation with life-sized humanoid robot: Kicking a wooden plate put on a pole with aiming through the VR-HMD

In this paper, we add and test two extentions to the previous approach [13]. One is introducing swing foot landing time delay into LIP based restriction, and this enables us controling swing foot movement more safely in the 3D space. The other is online trajectory smoothing methods in the joint angle space with spline interpolation to ensure the velocity safety for our real robot actuators, and this enables us to execute more high speed whole body motion as much as the robot can. With these methods, we try to achieve extremely speedy and flexible master-slave operation like shown in the Fig.1, and we evaluate its performance compared to conventional one or ordinary human's performance.

II. Whole Body Master-Slave Tele-Operation System with Virtual Reality Ware

In our study, we constructed an experimental system for real time whole body master-slave operation as shown in Fig.2. In recent years, Virtual Reality (VR) field is growing up, and we can easily feedback the robot's stereo image to the operator via VR Head Mount Display (HMD). For our system, we introduced "HTC Vive". HTC Vive system can measure the position and orientation of each HMD, controller, tracker by infrared laser measurement system called

Y. Ishiguro, K. Kojima, F. Sugai, S. Nozawa, Y. Kakiuchi K. Okada and M. Inaba are with Graduate School of Information Science and Technology The University of Tokyo, 7-3-1 Hongo, Bunkyo-Ku, 113-8656 Tokyo, Japan

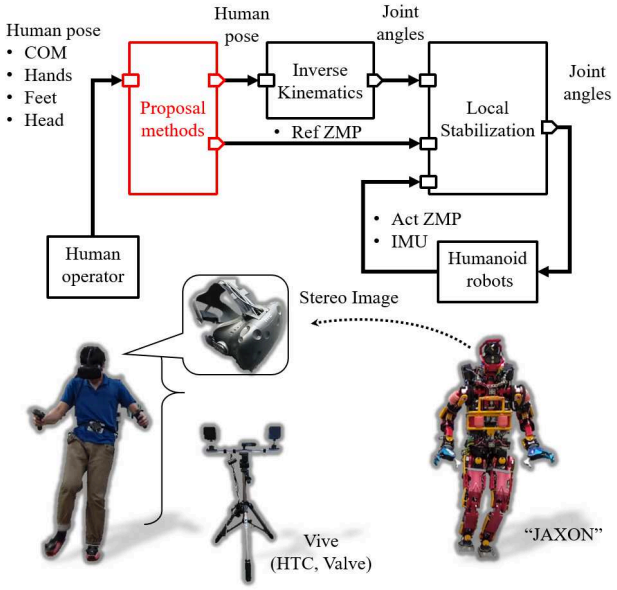

Fig. 2. Whole body master-slave system with optical human tracking: with some constraints about LIP dynamics, the operator can let the robot execute dynamic whole body motion with ease

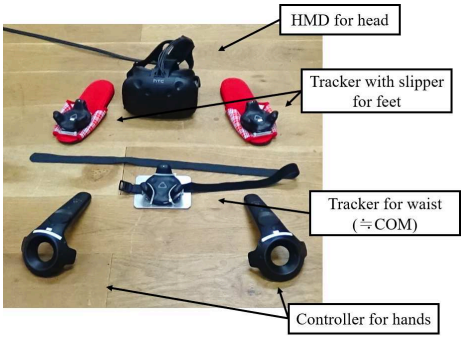

Fig. 3. HTC Vive HMD, controllers and trackers with some handmade extensions. The waist tracker is mounted with belt. The triggers on the hand controller are connected to the robot finger control. These devices act as low-cost motion capture system with enough precision

"lighthouse"[1]. By attaching those devices to the operator's body, we can get the pose of the operator's hands, feet, head and waist. Our extended devices for human posture tracking is shown in the Fig.3. Note that the COM position of the operator can not be measured directly in this way, so we regard the waist tracker position as the COM position. This replacement will cause several-centimeter error in the COM position measurement, however, with our proposed restrictions explained later, such an error does not matter in the robot operation. After processing input posture via our methods, modified end effector pose and COM position are passed to Inverse Kinematics (IK) solver and the generated joint angles are input to bipedal stabilization algorithm [16]. The stabilization process act as external disturbance absorber using actual foot force sensor value and reference Zero Moment Point (ZMP) trajectory. By assuming the robot and human dynamics ad LIP, we generate the reference ZMP by double differentiating the input COM position according to the Eq.(1)∼(3).

$$\ddot{x} = \frac{g}{h}(x - x_{\mathrm{Z}}) \tag{1}$$

$$\ddot{y} = \frac{g}{h}(y - y_{\mathrm{Z}}) \tag{2}$$

$$\ddot{z} = \frac{f_{\mathrm{z}}}{m} - g \tag{3}$$

In the equations above, x, y, z are the COM position, $x_{\mathrm{Z}}, y_{\mathrm{Z}}$ are the ZMP position on the horizontal plane, h is the height of COM, m, g, f_{z} are the scalars of the total mass, gravity, vertical floor reaction force. We don't consider so much COM height displacement, we ignored the COM dynamics in Z axis discribed in the Eq.(3).

In the actual experiment explained later, we used life-sized high-power humanoid robot "JAXON [17]". JAXON has two feet actuated by high-power motor driver system, and its design is inherited from "STARO [18]" a life-sized high-power humanoid robot, also developed in our laboratory. JAXON has 33 DOF joints except hand finger joint, and upper body joints can drive up to about 4 rad/s and lower body ones are up to about 9 rad/s according to the designed specification. Its software system is constructed with RTM·ROS interoperation technology [19].

The multisense mounted on the JAXON's head can output stereo images with 1024×544 px at 15 fps[2] and the stereo images are feedbacked to the operator's HMD.

III. Safety Limitations for High Speed Whole Body Master-Slave System

A. COM state limitation based on DCM, CCM and estimated foot landing time delay

In our previous work [13], we introduced LIP model based COM state and support change restrictions, and we achieved dynamic bipedal locomotion with master-slave controlled humanoid robot. In this paper, we use the same methods again with some extensions. Thus, we explain our previous method below, and after that we explain about extended features.

First, we focused on the convex hull formed with the both sole region projected to the ground, and we named it "Predicted Support Region (PSR)". This concept is not complex at all, however, one unique feature is that the PSR is always formed with both sole region even if swing leg is in the air, and it is projected on the ground as shown in the Fig.4. In addition, we also focused on the Divergent Component of Motion (DCM) and Convergent Component

[1]The precision is said to be about 0.3 mm. The update frequency seems to be 30/90/1000 Hz when using with OpenGL/Vulkan/NoRendering

[2]Other resolution and fps modes are prepared, however resolution and fps are trade-off

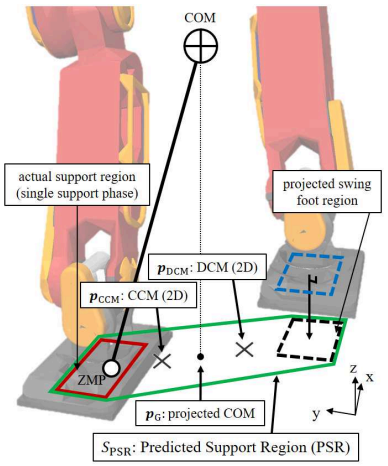

Fig. 4. Predicted Support Region: this region is formed with the both foot region even if the swing foot is in the air

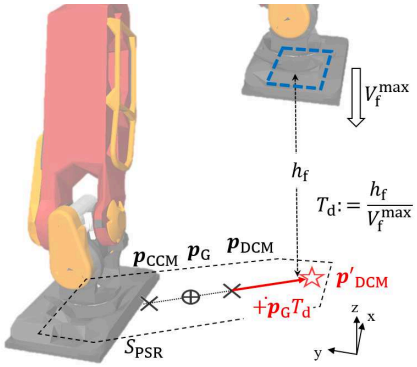

Fig. 5. Online COM velocity modification for bipedal robot: the COM velocity will be regulated when its $\boldsymbol{p}'_{\mathrm{DCM}}$ or $\boldsymbol{p}_{\mathrm{CCM}}$ go outside of the PSR. The $\boldsymbol{p}'_{\mathrm{DCM}}$ includes the delay of the swing foot landing, even if the swing foot is lifted highly, the robot can safely contact its swing foot.

of Motion (CCM) [20] in the 2D-plane.

$$\boldsymbol{p}_{\mathrm{DCM}} := \boldsymbol{p}_{\mathrm{G}} + \dot{\boldsymbol{p}}_{\mathrm{G}} \sqrt{\frac{h}{g}} \tag{4}$$

$$\boldsymbol{p}_{\mathrm{CCM}} := \boldsymbol{p}_{\mathrm{G}} - \dot{\boldsymbol{p}}_{\mathrm{G}} \sqrt{\frac{h}{g}} \tag{5}$$

The expression of the DCM in the 2D-plane is also known as Capture Point [21], and it can be utilized as a deceleration condition of COM velocity. We regarded the DCM and CCM as deceleration and acceleration conditions, and by keeping them inside the PSR at any time as shown in the Fig.5. Furthermore, by combining with auto foot landing function, which force the swing leg if ZMP goes out of the support leg region, we achieved non static COM movement with ensuring the feasibility of the bipedal motion. However, this restriction assumes that the swing foot is always near the ground plane, and the required time to land on the ground is assumed to be almost zero.

In this paper, we extend the position of the DCM according to the delay time of the swing foot landing as shown in the Eq.(6), and we aim to enable more flexible lower limb motions include unignorable swing foot height.

$$\boldsymbol{p}'_{\mathrm{DCM}} := \boldsymbol{p}_{\mathrm{G}} + \dot{\boldsymbol{p}}_{\mathrm{G}} (\sqrt{\frac{h}{g}} + T_{\mathrm{d}}) \tag{6}$$

As shown in the Eq.(6), we insert a delay time T_{d} that is required to let the swing foot land on the ground. Theoretically, because the dynamics of DCM is affected by ZMP position, future position of DCM is unpredictable in real time. Thus, we approximately extend the current DCM position $\boldsymbol{p}_{\mathrm{DCM}}$ by current COM velocity times swing foot landing delay time $\dot{\boldsymbol{p}}_{\mathrm{G}} T_{\mathrm{d}}$, and we update these values sequentially. Note that we set T_{d} simply as Eq.(7).

$$T_{\mathrm{d}} := \frac{h_{\mathrm{f}}}{V_{\mathrm{f}}^{\max}} \tag{7}$$

h_{f} is the current swing foot height, and $V_{\mathrm{f}}^{\max}$ is the maximum average vertical velocity of the swing foot estimeted roughly with hardware specification. By substituting $\boldsymbol{p}'_{\mathrm{DCM}}$ for $\boldsymbol{p}_{\mathrm{DCM}}$, we force the COM velocity to wait the swing foot complete ground contact. As common limitations among this extended LIP dynamics restriction and previous one [13], the robot is assumed to be standing on a 2D plane, and even if the LIP dynamics allowed, the full body multi-link dynamics is still ignored. External force disturbances are not also considered, hitting or pushing heavy objects can't be realized.

B. Sequential updated cubic spline interpolation to keep actuator velocity limit roughly

When we send a human motion to a humanoid robot, the hardware limitation of the actuators will be a problem first. To prevent excessive actuator stress caused by sudden acceleration or deceleration or discontinuous input, we must ensure the velocity continuity at least. That means, even if discontinuous trajectories are send online, the output trajectories must be smoothened to be continuous. In theory, actuator torque can be ensured its limitation in the motion planning phase, however in the case of online real time use, it is hard to include dynamics conditions into smoothing process, and available trajectory smoothing methods are limited. First, we can smoothen the trajectory with Low Pass Filter (LPF), however, when it comes to humanoid joint angle control, slowing down the specific joint is incorrect as shown in the top of Fig.6. In other words, we must ensure the consistency among all joint angle transitions to replay the commanded posture as it is. For that requirement, several interpolation methods e.x. polynomial interpolation are available. However, those interpolation approaches must to be set a certain constant interpolation time to reach target goal, the designed constant time delay could be too long or too short like shown in the middle of Fig.6.

In our system, we thought of setting the interpolation time to be variable depending on the actuator load, and we let the interpolation process recalculate the interpolation time and

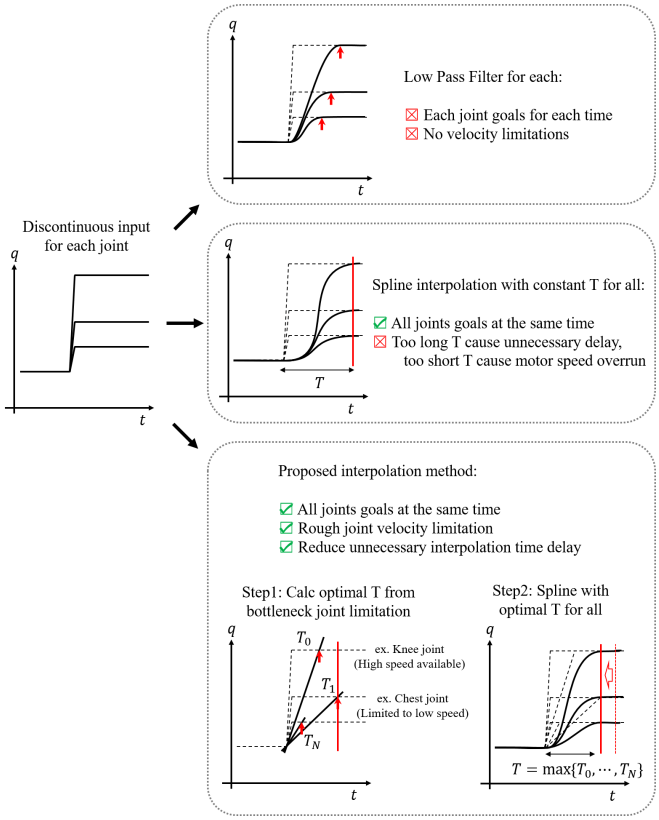

Fig. 6. Our proposed joint trajectory interpolation method: We set variable interpolation time T calculated from bottleneck joint speed

result trajectory at every control period. By applying the optimal time span for the all joint angle interpolations, we aim to keep both posture consistency and optimal interpolation for high speed motions.

When we set interpolation time span t=0∼T, The expression of the spline interpolation can be described as Eq.(8).

$$a_{\mathrm{N}}t^{\mathrm{N}} + \cdots + a_1 t + a_0 \tag{8}$$

$a_0 \cdots a_{\mathrm{N}}$ are coefficient defined after. Cubic spline interpolation is Eq.(9).

$$a_3 t^3 + a_2 t^2 + a_1 t + a_0 \tag{9}$$

As we can understand with double differentiating above, this curve has continuous velocity and continuous acceleration. When we set $q_{\mathrm{i}}, \dot{q}_{\mathrm{i}}$ as current i-th joint angle and velocity and $q_{\mathrm{i}}^{\mathrm{ref}}, \dot{q}_{\mathrm{i}}^{\mathrm{ref}}$ as target i-th joint angle and velocity, $a_0 \cdots a_3$ are defined as below.

$$a_0 = q_{\mathrm{i}} \tag{10}$$

$$a_1 = \dot{q}_{\mathrm{i}} \tag{11}$$

$$a_2 = \frac{-3q_{\mathrm{i}} + 3q_{\mathrm{i}}^{\mathrm{ref}} - 2\dot{q}_{\mathrm{i}}T - \dot{q}_{\mathrm{i}}^{\mathrm{ref}}T}{T^2} \tag{12}$$

$$a_3 = \frac{2q_{\mathrm{i}} - 2q_{\mathrm{i}}^{\mathrm{ref}} + \dot{q}_{\mathrm{i}}T + \dot{q}_{\mathrm{i}}^{\mathrm{ref}}T}{T^3} \tag{13}$$

For the real time sequential update, we can not know the safe velocity at the end time, we always set $\dot{q}_{\mathrm{i}}^{\mathrm{ref}} = 0$.

Furthermore, we set variable interpolation time span T to prevent velocity limitation over. When i-th actuator maximum average velocity and acceleration are $V_{\mathrm{i}}^{\mathrm{avg}}, A_{\mathrm{i}}^{\mathrm{avg}}$, we set T as Eq.(15).

$$T_{\mathrm{i}} = \max\{\frac{|q_{\mathrm{i}}^{\mathrm{ref}} - q_{\mathrm{i}}|}{V_{\mathrm{i}}^{\mathrm{avg}}}, \frac{|\dot{q}_{\mathrm{i}}|}{A_{\mathrm{i}}^{\mathrm{avg}}}\} \tag{14}$$

$$T = \max\{T_0, \cdots, T_{\mathrm{N}-1}\} \tag{15}$$

N is number of all joints in the robot. The designed expression of T_{i} means that this variable may take a bottleneck one from a required time to reach the goal with $V_{\mathrm{i}}^{\mathrm{avg}}$ or required time to brake with $A_{\mathrm{i}}^{\mathrm{avg}}$. This expression doesn't tell us accurate required time to reach goal state with the cubic spline formulation, but tell us roughly estimated required reach time. Why we don't use analytical solution of the spline formula as T_{i} is, with considering current state and goal state and joint angle limitation, we afraid the required reach time estimation goes more complex. By choosing the maximum T_{i} as T, and apply it commonly to the all joints as shown in the Fig.6, we keep joint velocity and acceleration condition and posture validity.

IV. Experiments of High Speed Whole Body Master-Slave Operation

We conducted several experiments with our proposed methods. First, we checked how much the dynamic COM movement and footworks contribute to the total performance. We sent a simple handmade dummy motion composed of discontinuous target pose shown in the Tab.I, and let the robot track to the target posture as fast as he can. In the Tab.I, "LF", "RF", "LH" and "RH" mean left foot, right foot, left hand and right hand. Note that the vectors $(\Delta x, \Delta y, \Delta z)$ shown in the Tab.I mean increments from the initial position in the initial standing posture.

As shown in the Fig.9, even if the discontinuous end effector reference targets were input as shown in Tab.I, spline interpolation with rough velocity limitation process smoothened the whole body joint angles after processing Inverse Kinematics. Fig.10 is the joint angle velocity calculated by differentiation of the Fig.9. Since maximum average joint velocity was set to 4.0 rad/s, even if the discontinuous input comes, the absolute value of joint angle velocity was almostly regulated under the 4.0 rad/s. Note that this velocity limitation regulates with average velocity value $V_{\mathrm{i}}^{\mathrm{avg}}$, actual output velocity after smoothing may excess $V_{\mathrm{i}}^{\mathrm{avg}}$ a bit.

The photographs of this two comparison results are shown in the Fig.7 and Fig.8. In the Fig.7, we disabled the COM movement and foot support change. On the other hand, we applied our proposed methods and the result is shown in the Fig.8. In the Fig.7, this master-slave control system is similar to conventional COM-static system, and the comparison of the horizontal swing hand trajectory between this two cases is shown in the Fig.11.

The two linear arrows in the Fig.11 mean reference swing hand position transitions defined in the Tab.I, and as we can

TABLE I

DISCONTINUOUS DUMMY INPUT LIKE TENNIS SWING TO CHECK INTERPOLATION VALIDITY AND PERFORMANCE IMPROVEMENT

Time [s]	COM $(\Delta x, \Delta y, \Delta z)$ [m]	LF $(\Delta x, \Delta y, \Delta z)$ [m]	RF $(\Delta x, \Delta y, \Delta z)$ [m]	LH $(\Delta x, \Delta y, \Delta z)$ [m]	RH $(\Delta x, \Delta y, \Delta z)$ [m]
0.0	($\pm$ 0, -0.1, $\pm$ 0)	($\pm$ 0, +0.2, $\pm$ 0)	($\pm$ 0, $\pm$ 0, $\pm$ 0)	($\pm$ 0, $\pm$ 0, $\pm$ 0)	(+0.3, -0.5, $\pm$ 0)
2.0	($\pm$ 0, +0.3, $\pm$ 0)				
3.0				(-0.2, 0.5, $\pm$ 0)	(+0.3, +1.2, $\pm$ 0)

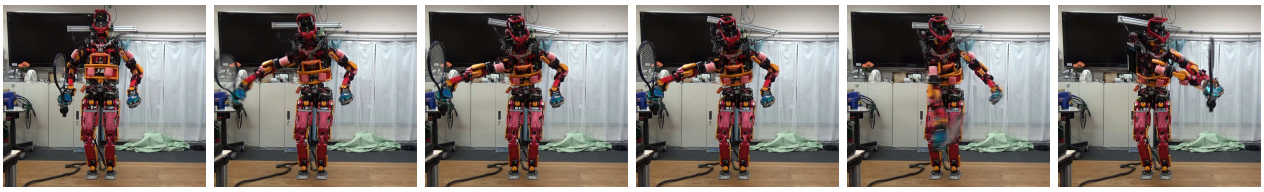

(a) t=0.0 (b) t=0.5 (c) t=1.0 (d) t=3.0 (e) t=3.5 (f) t=4.0

Fig. 7. Executing sample tennis swing motion without COM movement and footwork: COM position is constantly constrained to be initial position

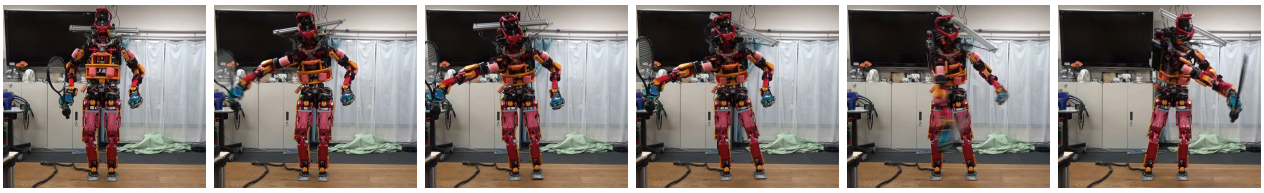

(a) t=0.0 (b) t=0.5 (c) t=1.0 (d) t=3.0 (e) t=3.5 (f) t=4.0

Fig. 8. Executing sample tennis swing motion with COM movement and footwork: Due to the COM and left foot movement in Y-direction, right hand can swipe more wide space

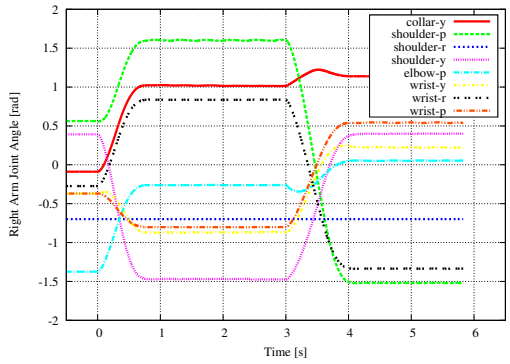

Fig. 9. Interpolated joint angle trajectory of right arm joints.

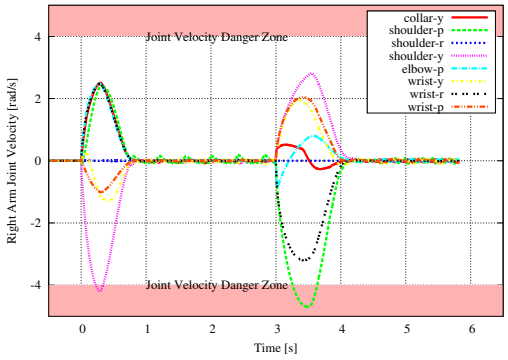

Fig. 10. Velocity plot by differentiation of Fig.9 right arm joints.

see in this figure, without COM movement and footwork, the robot manipulator reached reachability limit and could not reach to the target position. On the other hand, with COM movement and footwork, the swing hand reached target position successfully, and in this comparison, 30% expansion of the reachable range was confirmed in Y-Axis. The expansion of reachable range can be also seen in the comparison between Fig.7(f) and Fig.8(f). In terms of the end effector velocity norm, a comparison between the two cases is shown in the Fig.12. Unfortunately, the velocity improvement appeared in this experiment was only about 10% in the swing phase at 3$\sim$4 s.

With this master-slave system, when the operator mounts the HMD and swings the hand controller toward the ball with watching the stereo image, the robot also performs racket swing and succeed to hit the top-hooked ball as shown in the Fig.13. However, as a honest opinion, we felt a bit hard to catch up the speedy ball trajectory with 15 fps stereo image refresh rate.

Analysed from the video frames in the Fig.14, with considering the ball diameter is 6.7 cm, the shot speed seems to be about 3.3 m/s. An ordinary tennis ball rally speed is said to be over 120 km/h = 33 m/s, and our shot speed is 10% of that unfortunately. In the conventional research with offline optimization approach [22], they achieved 14.6 m/s racket speed, and our experiment achieved 23% of them with online master-slave approach.

We also conducted high kick motion task shown in the

(a) t=0.0 (b) t=1.0 (c) t=2.0 (d) t=2.3 (e) t=2.7 (f) t=3.0

Fig. 13. Tennis swing experiment with a racket and image feedback to the operator

(a) t=0.0 (b) t=12.0 (c) t=14.5 (d) t=15.0 (e) t=16.0 (f) t=17.0

Fig. 15. High speed high kick motion execution with real time whole body master-slave humanoid system: the target wooden plate is put on the 60 cm height pole fixed on the ground

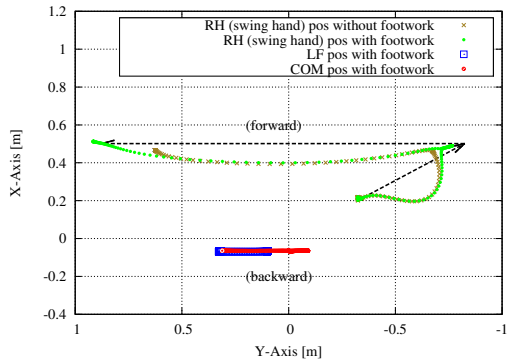

Fig. 11. Comparison with the swing hand horizontal trajectory of the COM-static system and our proposed system

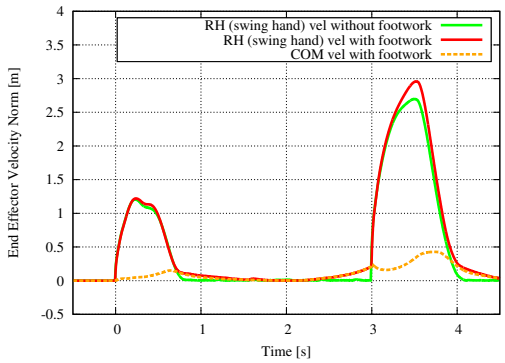

Fig. 12. Comparison with the swing hand velocity norm of the two system: without COM movement and footwork vs with COM movement and footwork

Fig.15 as another dynamic motion example. This motion includes unignorable swing foot height and risks in the swing foot lifting and landing. Due to the restriction explained in the Subsection.III-A, our robot can perform safe COM movement and foot landing, and we succeeded in kicking the target plate put on 60 cm height.

V. Conclusion

In this paper, we proposed

1) extended COM velocity restriction that can treat unignorable swing foot height.
2) sequential cubic spline interpolation method which keeps actuator velocity limit roughly.

We conducted real time whole body master-slave experiment with life-sized humanoid robot and evaluated the performance. In the tennis swing experiment, our proposed system can

1) expand the reachable space by 30% with footwork and COM movement.
2) speed up the end effector velocity by 10% with footwork and COM movement.
3) achieve 3.3 m/s shot speed which is equivalent for 10% of ordinary human's one and 23% of conventional offline approach [22].
4) achieve high kick motion toward over 60 cm height without falling down.

We think the performance difference between this report and previous offline approach [22] comes from the difference of online or offline and the difference of work space or joint space. Offline optimization can utilize richer information about reference trajectory includes future trajectory. Joint space optimization can utilize maximum performance of each joint easily compared to IK based motion generation. Actually, the offline approach [22] and this report used same robot hardware and maximum joint speed configuration 4 rad/s, however, the offline joint space optimization utilized more joints e.g. chest, lower limbs to accelerate the swing hand, and the maximum racket speed exceeds ours. In

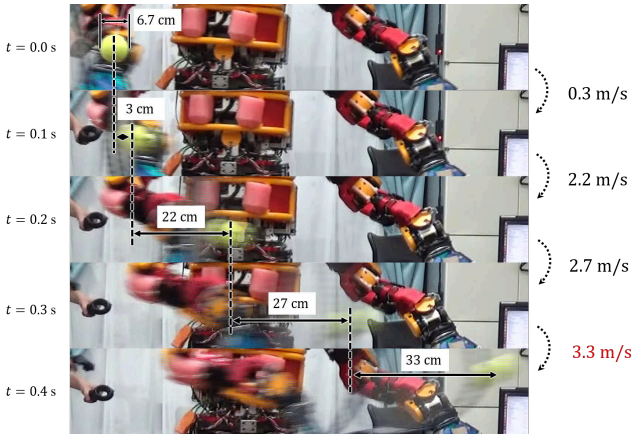

Fig. 14. Shot speed estimation with video frame: Ball diameter is 6.7 cm, screenshot is every 0.1 s, the maximum shot speed was 3.3 m/s

addition, to catch up the human performance, we think we are required to address some other factors e.g. muscle elasticity.

However we think no other master-slave system without ours can reproduce such dynamic motion in real time, and we hope our report will contribute to the field of humanoid tele-operation and tele-existence.

As our future works, we are planning to improve update rate of stereo vision system and response of manipulation, and we are aiming to achieve real time tennis rally with improved swing speed as fast as human. Furthermore, to operate the system with more ease, we must implement self collision avoidance not only acts as emergency stop but also enables continuous motion execution without stopping during operation.

REFERENCES

[1] Neo Ee Sian, Kazuhito Yokoi, Shuuji Kajita, Fumio Kanehiro, and Kazuo Tanie. Whole body teleoperation of a humanoid robot-development of a simple master device using joysticks. In *Intelligent Robots and Systems, 2002. IEEE/RSJ International Conference on*, Vol. 3, pp. 2569–2574. IEEE, 2002.

[2] J. Chestnutt, P. Michel, K. Nishiwaki, J. Kuffner, and S. Kagami. An intelligent joystick for biped control. In *Proceedings 2006 IEEE International Conference on Robotics and Automation, 2006. ICRA 2006.*, pp. 860–865, May 2006.

[3] Susumu Tachi, Kiyoshi Komoriya, Kazuya Sawada, Takashi Nishiyama, Toshiyuki Itoko, Masami Kobayashi, and Kozo Inoue. Telexistence cockpit for humanoid robot control. *Advanced Robotics*, Vol. 17, No. 3, pp. 199–217, 2003.

[4] M. Stilman, Koichi Nishiwaki, and Satoshi Kagami. Humanoid tele-operation for whole body manipulation. In *2008 IEEE International Conference on Robotics and Automation*, pp. 3175–3180, May 2008.

[5] M. Riley, A. Ude, K. Wade, and C. G. Atkeson. Enabling real-time full-body imitation: a natural way of transferring human movement to humanoids. In *2003 IEEE International Conference on Robotics and Automation (Cat. No.03CH37422)*, Vol. 2, pp. 2368–2374 vol.2, Sept 2003.

[6] K. Hongo, M. Yoshida, Y. Nakanishi, I. Mizuuchi, and M. Inaba. Development of bilateral wearable device "kento" for control robots using muscle actuator modules. In *RO-MAN - The 18th IEEE International Symposium on Robot and Human Interactive Communication*, pp. 897–902, Sept 2009.

[7] C. L. Fernando, M. Furukawa, T. Kurogi, S. Kamuro, K. sato, K. Minamizawa, and S. Tachi. Design of telesar v for transferring bodily consciousness in telexistence. In *2012 IEEE/RSJ International Conference on Intelligent Robots and Systems*, pp. 5112–5118, Oct 2012.

[8] Francisco-Javier Montecillo-Puente, Manish N Sreenivasa, and Jean-Paul Laumond. On real-time whole-body human to humanoid motion transfer. In *ICINCO (2)*, pp. 22–31, 2010.

[9] J. Koenemann, F. Burget, and M. Bennewitz. Real-time imitation of human whole-body motions by humanoids. In *2014 IEEE International Conference on Robotics and Automation (ICRA)*, pp. 2806–2812, May 2014.

[10] Louise Penna Poubel, Sophie Sakka, Denis Ćehajić, and Denis Creusot. Support changes during online human motion imitation by a humanoid robot using task specification. In *International Conference on Robotics and Automation (ICRA)*, pp. 1782–1787. IEEE, 2014.

[11] A. Wang, J. Ramos, J. Mayo, W. Ubellacker, J. Cheung, and S. Kim. The hermes humanoid system: A platform for full-body teleoperation with balance feedback. In *Humanoid Robots (Humanoids), 2015 IEEE-RAS 15th International Conference on*, pp. 730–737, Nov 2015.

[12] Yasuhiro Ishiguro, Tatsuya Ishikawa, Kunio Kojima, Fumihito Sugai, Shunichi Nozawa, Yohei Kakiuchi, Kei Okada, and Masayuki Inaba. Online Master-Slave Footstep Control for Dynamical Human-Robot Synchronization with Wearable Sole Sensor. In *Proceedings of the 2016 IEEE-RAS International Conference on Humanoid Robots (Humanoids 2016)*, pp. 864–869, November 2016.

[13] Yasuhiro Ishiguro, Kunio Kojima, Fumihito Sugai, Shunichi Nozawa, Yohei Kakiuchi, Kei Okada, and Masayuki Inaba. Bipedal Oriented Whole Body Master-Slave System for Dynamic Secured Locomotion with LIP Safety Constraints. In *2017 IEEE/RSJ International Conference on Intelligent Robots and Systems (IROS2017)*, September 2017.

[14] Kazuhisa Mitobe, Genci Capi, and Yasuo Nasu. Control of walking robots based on manipulation of the zero moment point. *Robotica*, Vol. 18, No. 06, pp. 651–657, 2000.

[15] Tomomichi Sugihara, Yoshihiko Nakamura, and Hirochika Inoue. Real-time humanoid motion generation through zmp manipulation based on inverted pendulum control. In *Robotics and Automation, 2002. Proceedings. ICRA'02. IEEE International Conference on*, Vol. 2, pp. 1404–1409. IEEE, 2002.

[16] S. Kajita, M. Morisawa, K. Miura, S. Nakaoka, K. Harada, K. Kaneko, F. Kanehiro, and K Yokoi. Biped walking stabilization based on linear inverted pendulum tracking. In *Intelligent Robots and Systems (IROS)*, pp. 4489–4496. IEEE, 2010.

[17] K. Kojima, T. Karasawa, T. Kozuki, E. Kuroiwa, S. Yukizaki, S. Iwaishi, T. Ishikawa, R. Koyama, S. Noda, F. Sugai, S. Nozawa, Y. Kakiuchi, K. Okada, and M. Inaba. Development of life-sized high-power humanoid robot jaxon for real-world use. In *Humanoids*, pp. 838–843, Nov 2015.

[18] Y. Ito, S. Nozawa, J. Urata, T. Nakaoka, K. Kobayashi, Y. Nakanishi, K. Okada, and M. Inaba. Development and verification of life-size humanoid with high-output actuation system. In *ICRA*, pp. 3433–3438, May 2014.

[19] Yohei Kakiuchi, Kunio Kojima, Eisoku Kuroiwa, Masaki Murooka, Shintaro Noda, Iori Kumagai, Ryohei Ueda, Fumihito Sugai, Shunichi Nozawa, Kei Okada, and Masayuki Inaba. Development of Humanoid Robot System for Disaster Response Through Team NEDO-JSK's Approach to DARPA Robotics Challenge Finals. In *Humanoids2015*, pp. 805–810, 2015.

[20] Toru Takenaka, Takashi Matsumoto, and Takahide Yoshiike. Real time motion generation and control for biped robot - 1st report: Walking gait pattern generation-. *2009 IEEE/RSJ International Conference on Intelligent Robots and Systems*, pp. 1084–1091, 2009.

[21] J. Pratt, J. Carff, S. Drakunov, and A. Goswami. Capture Point: A Step toward Humanoid Push Recovery. In *2006 6th IEEE-RAS International Conference on Humanoid Robots*, pp. 200–207, Dec 2006.

[22] R. Terasawa, S. Noda, K. Kojima, R. Koyama, F. Sugai, S. Nozawa, Y. Kakiuchi, K. Okada, and M. Inaba. Achievement of dynamic tennis swing motion by offline motion planning and online trajectory modification based on optimization with a humanoid robot. In *2016 IEEE-RAS 16th International Conference on Humanoid Robots (Humanoids)*, pp. 1094–1100, Nov 2016.